Full length article

Optical pulse dynamics in fiber links with dispersion compensation

Ildar Gabitov [a,c], Elena G. Shapiro [b], Sergei K. Turitsyn [b,c,1]

[a] *L.D. Landau Institute for Theoretical Physics, Kosygin St. 2, 117940 Moscow, Russia*
[b] *Institute of Automatics and Electrometry, University Prospect 1, 630090 Novosibirsk, Russia*
[c] *Institut für Theoretische Physik I, H.-H.-Universität Düsseldorf, Universitätsstr. 1, 40225 Düsseldorf, Germany*

Abstract

We examine optical pulse propagation in a transmission system with periodical pulse amplification and dispersion compensation both numerically and by a variational method. We confirm by direct numerical simulations the validity of the concept of a "breathing" soliton, which we previously proposed. We demonstrate that the sign of the residual dispersion is responsible for the stability of the pulse stream.

1. Introduction

The main problem of high-bit-rate transmission in optical fiber links is the limitation caused by the fiber chromatic dispersion. Among the numerous methods proposed as solutions of this problem, two approaches are presently in the focus of intensive investigations worldwide. One of these approaches is soliton transmission, where the dispersion is balanced by the Kerr nonlinearity. Another approach is direct dispersion compensation for linear pulse propagation.

The first approach to overcome fiber chromatic dispersion, the soliton transmission, has already exhibited its potential in long-haul, high-speed communications. Recent progress in the fabrication of er-

bium-doped fiber amplifiers with very high characteristics and of low-dispersion optical fibers clearly demonstrated the impressive potential of long-distance, soliton-based optical communication systems (see e.g. Refs. [1–4]). Pulse propagation in optical transmission lines that employ these new devices can be described by the theory of guiding-center (average) solitons [1,5,6]. This theory is valid for bit-rates for which the amplifier spacing is shorter than the soliton period, and, on the scale of the amplifier distance, both the dispersion and the nonlinearity can be treated as perturbations. Thus, at the leading order, only the fiber losses and the periodic amplification are significant factors. They cause oscillations of the amplitude, while the form of the pulse remains unchanged. The dispersion and the nonlinearity come into play only at much longer distances that cover many amplifier spacings.

Advantages of the soliton approach include the natural compensation of the dispersion by the nonlin-

---

[1] E-mail: turitsyn@xerxes.thphy.uni-duesseldorf.de.

earity, the stability and robustness of solitons, and the almost negligible error-rate in multy-channel transmissions along distances of tens of thousands of kilometers [4]. All of these advantages result in the soliton technique yielding a very high capacity of data transmission in single-frequency channels.

The second approach to overcome fiber chromatic dispersion is based on linear methods, which also significantly enhance the respective transmission capacity. Several techniques may be used for this purpose. The most practical of these techniques consists of periodically incorporating into the optical system pieces of optical fibers with high dispersion of sign opposite to that of the remaining transmission line [7]. Another technique that could potentially be applied to achieve the same goal would use chirped fiber gratings (see for a review Ref. [8]), which allow the dispersion of 500 ps/nm or even more to be compensated by a grating fiber of a few decimeters in length. This second technique can be considered as "lumped" dispersion compensation. A third, as yet undeveloped but potentially even more efficient technique would consist of using the semiconductor waveguide device described in Ref. [9].

Dispersion compensation is a simple and effective technique with many attractive features: it is compatible with the present concept of the all-optical transparency of the system, it is cascadable, all the system components are commercially available, and it is very effective both in the "return-to-zero" (RZ) and the "non-return-to-zero" (NRZ) signal formats. The dispersion compensation technique has been identified in recent experiments [10–15] as a promising approach to increasing transmission capacity in communication systems that use standard monomode fibers (SMF) both in unrepeated transmission and cascaded systems. Thus, this approach is ideally suited for upgrading the existing optical communication networks that use SMF with in-line erbium-doped fiber amplifiers operating in the 1550 nm optical window.

In any practically-implemented optical network, it will not be possible to completely compensate for all the dispersion in each element. Therefore, there will always remain some residual dispersion. Furthermore, the amplitude of the signal is bounded from below by the bit-error-rate standards, namely, if the amplitude is too small, the relative contribution of the surrounding noise to the bit-error-rate becomes too large. Thus, on the scale of the amplification distance, pulse propagation can be considered as linear, and the pulse's amplitude and width will experience oscillations due to the variation of dispersion, losses, and periodic amplification. On the longer scale of the complete transmission line, however, the nonlinearity and the residual dispersion do have to be taken into account, and this question has been recently investigated in Refs. [16–23]. The theory of this process was developed in Refs. [16,17,20], where it was shown that in several particular cases the leading order nonlinear correction that results from the dispersion and the nonlinearity is described by the Nonlinear Schrödinger equation. As a result, Gabitov et al. [16,17] proposed the concept of a "breathing" soliton in dispersion-compensated optical transmission lines. It has been discovered in Ref. [19] that the resulting asymptotic pulse is close to the Gaussian shape and has energy well above that of the soliton of the average dispersion. Pulse dynamics in the NLS equation with the dispersion varying as $\sin(kz)$ has been studied in Refs. [21,22]. Dispersion-allocated soliton transmission line using dispersion-shifted nonsoliton fibers has been suggested recently in Ref. [23]. Numerical simulations of the soliton transmission in short standard monomode fiber (SMF) systems upgraded by dispersion compensation have been performed in Ref. [18]. It has been shown that 10 Gbit/s transmission over 200 km is possible with a 36 km amplifier spacing. A piece of a dispersion compensating fiber (DCF) allows a complete recovery of the pulse width after the dispersive broadening due to the high dispersion of the SMF at 1550 nm.

Of the two approaches just described that can be used to overcome fiber chromatic dispersion, the linear dispersion-compensation approach is the more practical one. This is because it is more in tune with the characteristics of the already existing optical transmission networks, while the soliton approach has one major practical disadvantage that can be explained as follows: Most of the currently operating fiber links consist of SMF's with approximately 17 ps/nm × km dispersion in the third optical window (about 1550 nm). In these fiber links, electro-optical signal regenerators are usually placed at intervals of a few tens of kilometers. In any upgrade, these

regenerators will be replaced by in-line (lumped) optical amplifiers. These are erbium-doped fiber amplifiers that operate in the 1550 nm optical window. Now, any network upgrade should boost the data transmission in this window to the rate of at least 10 Gbit/s. At such a high rate, the associated soliton periods in SMF's are of the same order of magnitude as the amplifier spacing [18,24]. This causes a resonance, $Z_{sol} \approx Z_a$, which results in the destruction of the soliton data stream. The guiding-center soliton concept thus cannot be applied in this particular case.

In this paper we use a variational approach and numerical computations to study optical pulse propagation in realistic optical transmission systems that apply the dispersion compensation technique. We show that a "breathing" averaged optical pulse, which combines the advantages of the soliton approach with those of the dispersion compensation technique, can be used for describing optical data transmission in such systems. We derive an effective approximate model for the pulse dynamics by assuming that the nonlinear effects and the residual dispersion cause very slow evolution of this dynamics.

2. The modeling and the numerical computations

We consider a transmission line that consists of periodic sections, each of which includes a piece of a DCF, a piece of a transmission fiber, and a lumped optical amplifier, as shown in Fig. 1.

The DCF piece has normal dispersion D_- and length Z_c. The transmission fiber piece has anomalous dispersion D_+ and length $Z = Z_a - Z_c$. The average (residual) dispersion of the section is $D_{res} = [D_- Z_c + D_+ (Z_a - Z_c)]/Z_a$. In the experiment presented in Refs. [13,14], the total residual dispersion over a distance of 617 km in the $\lambda = 1550$ nm optical window was about 300 ps/nm; i.e., the dispersion is approximately equal to $\langle |D_{res}| \rangle \sim 0.5$ ps/(nm × km). In the numerical simulations [18], the residual dispersion $D_{res} \sim 6$ ps/(nm × km) was considered. In order for a "breathing" bright soliton to exist, the residual dispersion D_{res} must be positive (or the corresponding β_{2res} negative) [16].

There exist three characteristic dispersion scales in the system under consideration: the dispersion length Z_{DCF} that corresponds to the chromatic dis-
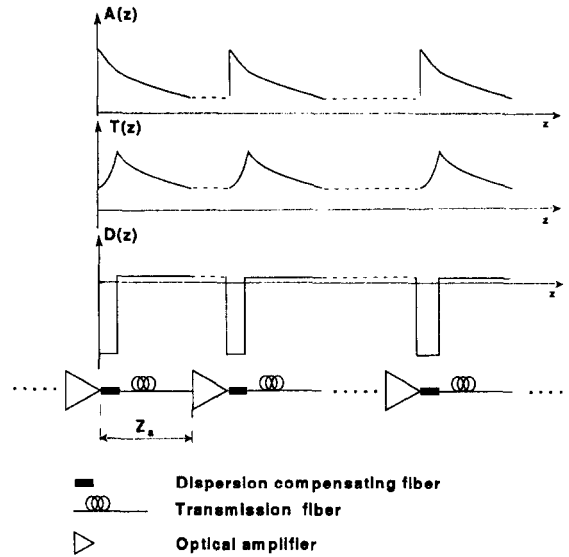

Fig. 1. Schematic diagram of the system design. Compensation is realized in each span between two amplifiers. Dispersion compensating fibers are followed by pieces of transmission fibers. Dispersion $d(z)$ is normalized to the SMF dispersion.

persion $D \simeq -(60-80)$ ps/(nm × km) of the DCF, the dispersion length of the transmission fiber Z_{dis}, and the dispersion length that corresponds to the residual dispersion of each section Z_{DR}.

The propagation of optical pulses through a cascaded-fiber transmission system is governed by the NLS equation

$$iA_z + \frac{Z_{NL}}{2Z_{dis}} d(z) A_{tt} + |A|^2 A = iG(z) A. \tag{1}$$

Here,

$$G(z)$$
$$= Z_{NL}\left(-\gamma + [\exp(\gamma Z_a) - 1] \sum_{k=1}^{N} \delta(z - z_k) \right),$$

$Z_{NL} = 1/(\sigma P_0)$ is the nonlinear length, $Z_{dis} = t_0^2/|\beta_2|$ is the dispersion length corresponding to the SMF, t_0 and P_0 are the width and the peak power of the incident pulse, β_2 is the group velocity dispersion for the SMF, σ is the coefficient of the nonlinearity, γ describes the fiber losses, Z_a is the amplification period, and $z_k = kz_a$ are the amplifier locations. The retarded time is normalized to the initial pulse width $t = T/t_0$, the envelope of the electric

field $E = E(T,Z)$ is normalized to the initial pulse power $|E|^2 = P_0|A|^2$, and the coordinate along the fiber z is normalized to the nonlinear length $z = Z/Z_{NL}$. The chromatic dispersion $d(z)$ is normalized here to the SMF dispersion coefficient.

2.1. Direct numerical simulations and the linear approximation

An optical pulse that propagates in a cascaded transmission system experiences periodic oscillations of its amplitude and width. At short distances, the pulse evolution can be approximately described as a linear process. As a pulse enters into a DCF part of the line, its width increases due to the dispersive broadening. The pulse also acquires a positive, dispersion-induced frequency chirp. After entering an SMF part of the line, the pulse compresses because the sign of the dispersion is reversed, and the condition for dispersion induced compression $\beta_2 C < 0$ is thus satisfied (see e.g. Ref. [25]). During the propagation in the fiber, the amplitude of the pulse is reduced due to the losses. Therefore, a pulse must be regenerated at the end of each section.

In cascaded systems, a basic section that includes a DCF, an SMF, and optical amplifier is periodically repeated. When the nonlinear effects and the residual dispersion are negligible, a pulse recovers its original form after passing through such a section. Indeed, the phase shift of the pulse corresponding to the Kerr effect is small over one cycle of this process. Therefore, the dispersion and the fiber losses are the leading-order effects. However, the small changes due to the Kerr effect do accumulate over several periodic segments of the transmission line, and thus at larger distances the Kerr nonlinearity may begin to come into play. The influence of the residual dispersion becomes important at the distance of $Z_{DR} \gg Z_a$, and alters the shapes of the pulses. The nonlinear length Z_{NL} is comparable to Z_{DR}. Therefore, in the description of the "slow" evolution of a pulse, one must take into account both the residual dispersion and the nonlinearity. Thus, "breathing" rapid oscillations of the pulse are accompanied by slow average changes of the pulse characteristics, which are due to the nonlinearity and the residual dispersion [16].

In order to illustrate the above-described "breathing" pulse dynamics, we here show the results of numerical simulations that we have performed directly on Eq. (1). We have integrated Eq. (1) numerically using the split-step method. The parameters typically used in the calculations are: the nonlinear
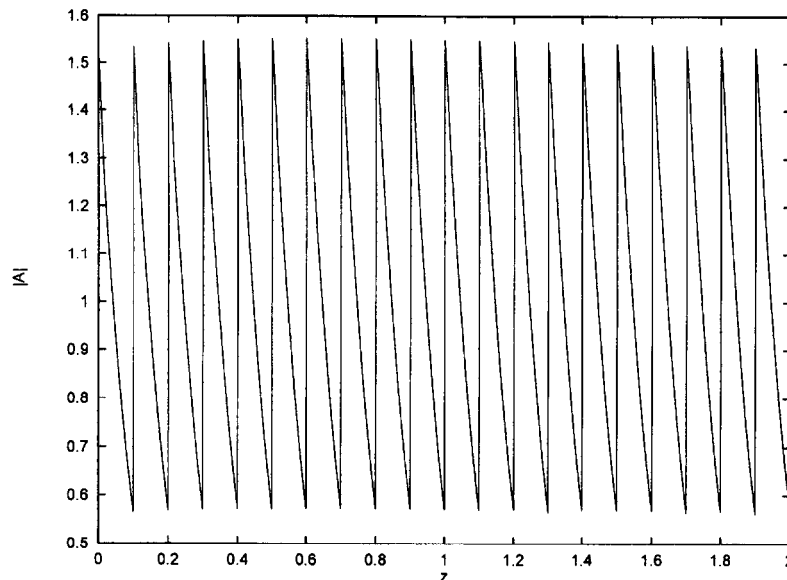

Fig. 2. Periodic oscillations of the amplitude. Eq. (1) was integrated numerically using the initial condition $A(0,t) = N/\cosh(t/T)$, $N^2 = (2\gamma Z_a)/[1 - \exp(-2\gamma Z_a)]$ and $T^2 = 0.3$. Residual dispersion was $\langle d \rangle = 0.3$.
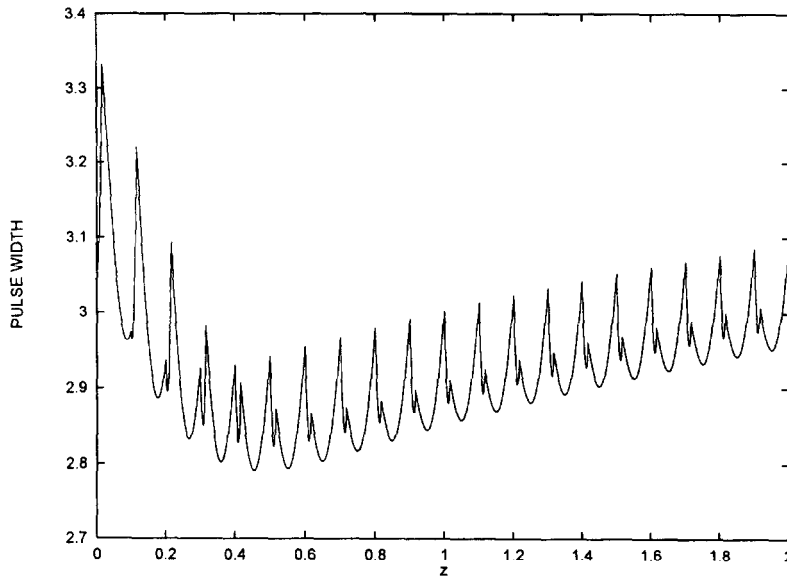
Fig. 3. Pulse width oscillations. Eq. (1) was integrated numerically using the initial condition $A(0,t) = N/\cosh(t/T)$, $N^2 = (2\gamma Z_a)/[1 - \exp(-2\gamma Z_a)]$ and $T^2 = 0.3$. Residual dispersion was $\langle d \rangle = 0.3$.

length $Z_{NL} = 360$ km, the amplifier spacing and the dispersion length $Z_a = Z_{dis} = 36$ km, the residual dispersion length $Z_{DR} \approx 360$ km, the length of the DCF $Z_c = 6$ km, the SMF dispersion $D_+ = 18$ ps/(nm × km), the DCF dispersion $D_- = -80$ ps/(nm × km), and the fiber loss coefficient in both the DCF's and the SMF's $\alpha = 0.25$ dB/km ($\gamma = 0.115\alpha$). The fiber loss coefficients in both the DCF's and the SMF's were chosen to be the same for simplicity, even though, in reality, the losses in
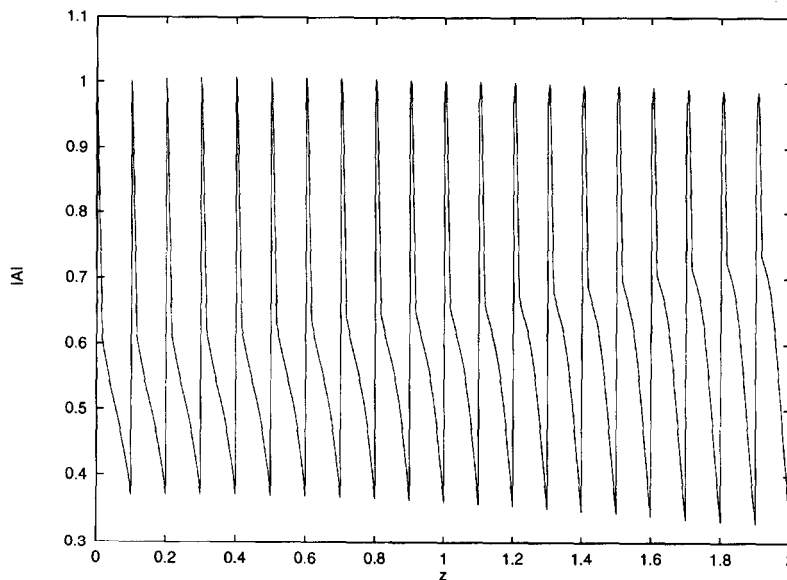

Fig. 4. Periodic oscillations of the amplitude. Eq. (1) was integrated numerically using the initial condition $A(0,t) = \exp(-t^2)$. Residual dispersion was $\langle d \rangle = 0.025$.
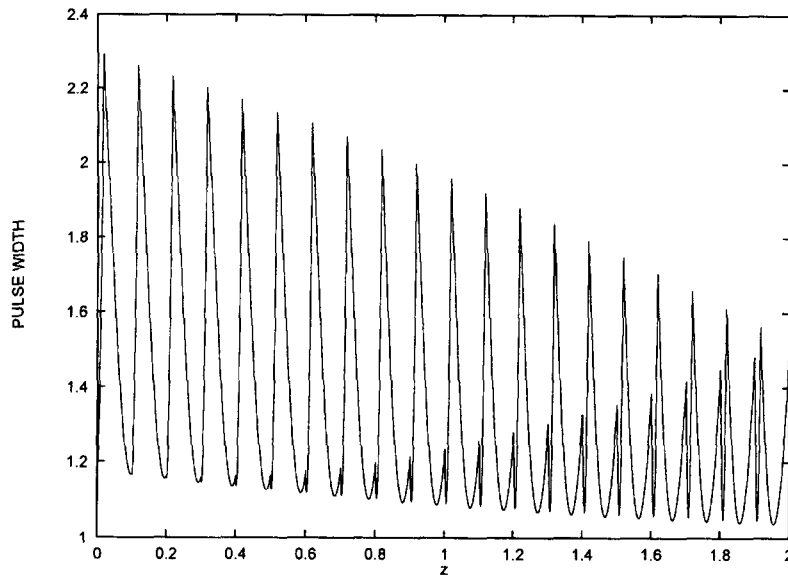
Fig. 5. Pulse width oscillations. Eq. (1) was integrated numerically using the initial condition $A(0,t) = \exp(-t^2)$. Residual dispersion was $\langle d \rangle = 0.025$.

the DCF's are higher than in the SMF's. The above parameters correspond to a pulse with peak power $P_0 \approx 2.2$ mW (in fact, in numerical simulation input power in dimensionless variables was larger than 1, therefore P_0 must be considered as normalizing parameter, rather than input pulse peak power) and width $t_0 = 26.8$ ps.

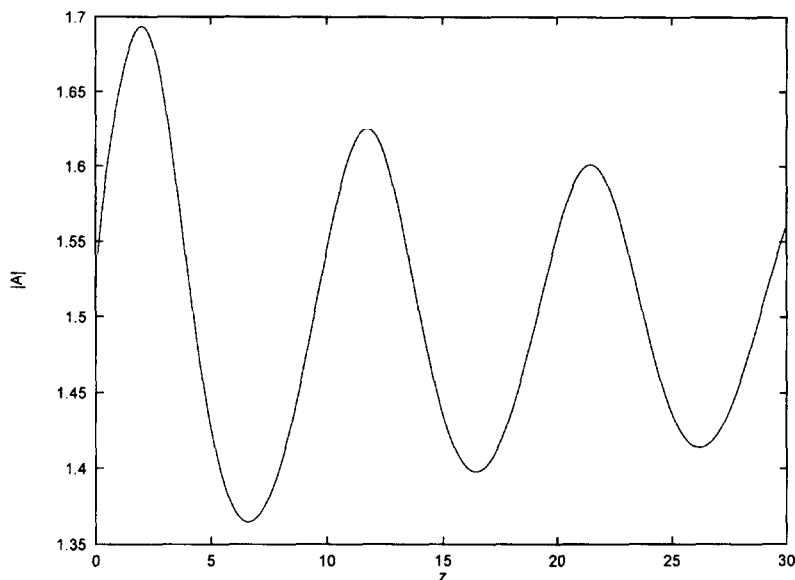In Figs. 2, 3, we present the evolution of an input

Fig. 6. Evolution of the envelope of pulse amplitude over many amplification periods. Envelope is shown for the pulse amplitude and width at the amplifiers ($z_k = kZ_a = 0.1k$ with $k = 1, 2, ...$). Initial conditions are $A(0,t) = N/\cosh(t)$, $N^2 = (2\gamma Z_a)/[1 - \exp(-2\gamma Z_a)]$ and $\langle d \rangle = 0.05$.
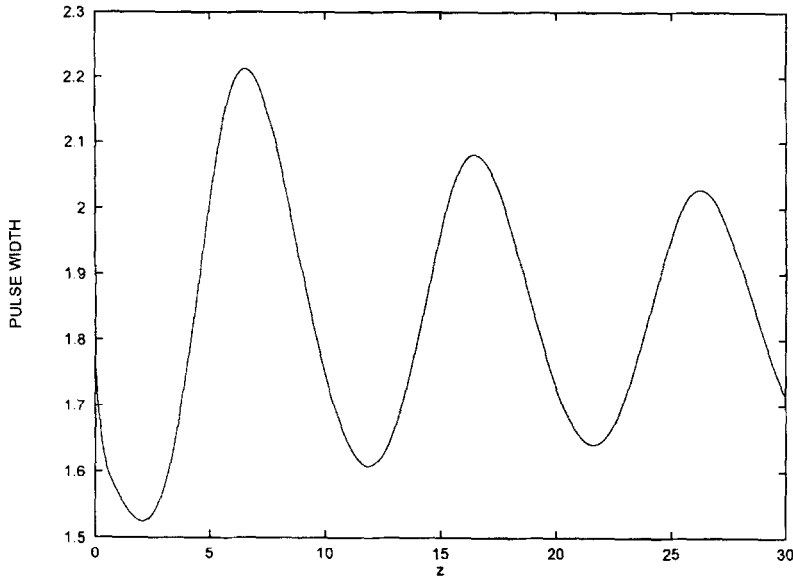
Fig. 7. Evolution of the pulse width over many amplification periods. Envelope is shown for the pulse amplitude and width at the amplifiers ($z_k = kZ_a = 0.1k$ with $k = 1, 2, ...$). Initial conditions are $A(0,t) = N/\cosh(t)$, $N^2 = (2\gamma Z_a)/[1 - \exp(-2\gamma Z_a)]$ and $\langle d \rangle = 0.05$.

pulse having the form $A(0,t) = N/\cosh(t/T)$, with $N^2 = 2\gamma Z_a/[1 - \exp(-2\gamma Z_a)]$ and $T^2 = 0.3$. The results shown in these figures illustrate that the pulse experiences periodic oscillations of the amplitude (Fig. 2) and the pulse width (Fig. 3). Figs. 2, 3 indicate that the breathing dynamics is accompanied by the reconstruction of a pulse due to the nonlinearity and the residual dispersion. The pulse evolves to
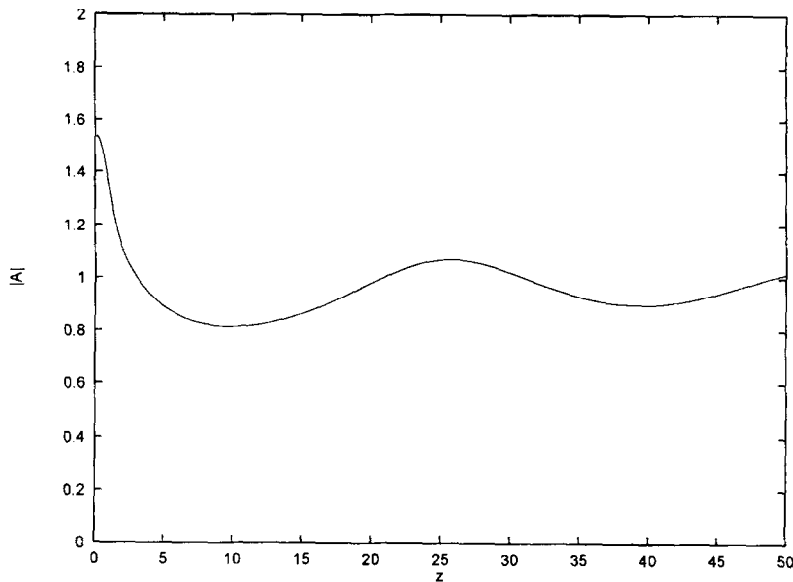

Fig. 8. Evolution of the envelope of pulse amplitude for the Gaussian input pulse $A(0,t) = 1.52 \exp(-t^2)$. Envelope is shown at the amplifiers ($z_k = kZ_a = 0.1k$ with $k = 1, 2, ...$); $\langle d \rangle = 0.05$.

a new state that manifests itself as breathing stable solitary wave. The speed of this reconstruction depends on residual dispersion value, initial pulse parameters and shape.

Due to the locally linear character of the rapid oscillations, the general features of the dynamics do not depend on the particular shape of the input signal. In particular, Figs. 4, 5 show the evolution of the Gaussian input pulse $A(0,t) = \exp(-t^2)$. The figures demonstrate that general features of the process do not depend significantly on the input pulse shape. The main feature of the initial stage is a transition of initial pulse to asymptotic stable state.

In Figs. 6, 7 it is demonstrated that after the first stage the input pulse experiences slow average oscillations of the amplitude and width and asymptotically evolves into a stable breathing soliton. We use here the term soliton, though the shape is not sech as for guiding-center solitons. Fig. 8 shows that for an initial Gaussian pulse average oscillations are rather small and have larger period in comparison with the sech input pulse. As was discovered in Ref. [19] the asymptotic pulse forming after many amplification periods is close to the Gaussian profile.

In the limit Z_a, $Z_{dis} \ll Z_{NL}$, one may treat the nonlinearity as a perturbation. At the lowest order,

the fast oscillations of the linear pulse amplitude and width are given by

$$A(z,t) = \int_{-\infty}^{+\infty} d\omega\, A_\omega$$
$$\times \exp\left(i\omega t - i\omega^2 \frac{Z_{NL}}{2Z_{dis}} \int_0^z \tilde{d}(\xi)\, d\xi \right).$$
$$(2)$$

Here, A_ω does not depend on z and is determined only by the initial pulse form. For a Gaussian input signal $A(0,t) = N \exp(-t^2)$, the linear oscillations are described by

$$A(z,t) = \frac{N}{\sqrt{\tau(z)}} \exp\left[-t^2/\tau^2(z) - iCt^2/\tau^2(z) \right. $$
$$\left. + i\Phi(z) \right],$$
$$(3)$$

where $\tau^2(z) = 1 + 16R^2(z)$, $dR/dz = d(z)Z_{NL}/(2Z_{dis})$, $C = 4R(z)$, and $\Phi = -0.5 \arctan(4R)$. The nonlinear effects become important on a scale which is large compared to Z_a, namely at distances proportional to Z_{NL}. The concept of the guiding-center soliton, which was introduced in Refs. [1,5], corresponds to the limit $Z_a \ll Z_{NL} = Z_{dis}$. In this work, we analyze the complementary regime with $Z_{NL} \gg Z_a = Z_{dis}$ [16,20]. The existence of the small parame-
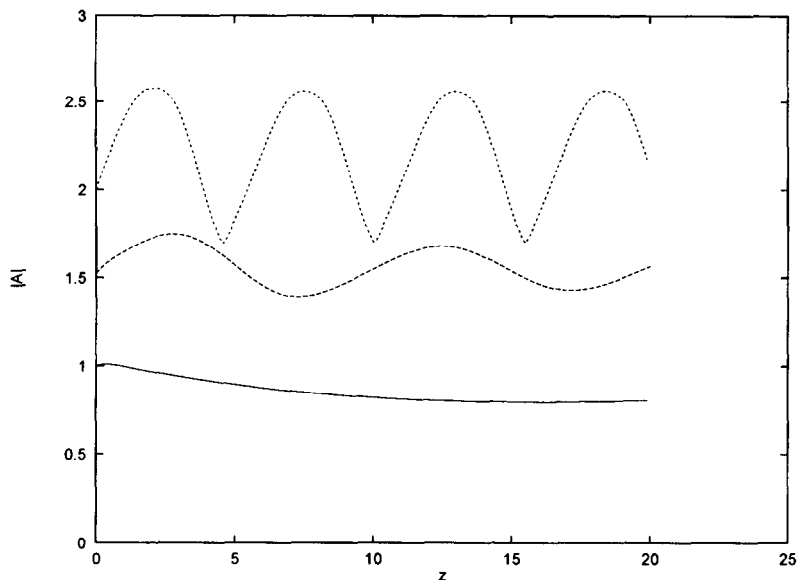

Fig. 9. Nonlinear effects. Pulse amplitude envelope (at maxima) evolution for different initial amplitudes. Initial pulse in the form $A(0,t) = B/\cosh(t)$ is considered. $B = 1$ (solid line); 1.52 (middle curve); 2 (upper curve) and $\langle d \rangle = 0.05$.

ters Z_{dis}/Z_{DR} and Z_a/Z_{NL} allows us to introduce a fast and a slow evolution scales [16]. The fast dynamics describes the oscillations of the amplitude and the shape of the pulse, while the slow dynamics describes the average changes due to nonlinear effects and the residual dispersion. Next, we study the role played by nonlinear effects on the optical pulse propagation. We would like to point out that the above exact solution (Eq. (3)) describing strong periodic oscillations of the pulse amplitude and width in the linear regime gives some explanation for the Gaussian shape of the asymptotic pulse found in Ref. [19].

In Figs. 9, 10 it is shown how nonlinearity influences propagation. In particular, the plots confirm our expectations that the deviations of the average dynamics from that described by the linearized equations are proportional to the strength of the nonlinearity. Evolution of the envelope of the pulse amplitude at the maxima is shown for different initial amplitudes. The plots show that for small nonlinearities the process is close to a linear one. For higher nonlinearity average changes become substantial and comparable with fast oscillations. The period of average oscillations decreases with increasing nonlin-

earity. For a Gaussian input signal the periods of slow average oscillations are larger than for corresponding sech input pulses.

2.2. The slow pulse dynamics and the variational approach

In what follows, we use a variational approach to derive a simple model that describes both the rapid oscillations and the average pulse evolution under the combined effects of the nonlinearity and the residual dispersion.

We begin by following Refs. [1,5] to transform A into a new function Q by taking out the rapid oscillations of the amplitude due to periodic amplification:

$$A = Q(t,z)\exp\left(\int_0^z G(z')\,\mathrm{d}z'\right). \tag{4}$$

The equation for Q reads

$$iQ_z + \frac{Z_{NL}}{2Z_{dis}}d(z)Q_{tt} + c(z)|Q|^2 Q = 0. \tag{5}$$

Here, $c(z) \equiv \exp(2\int_0^z G(z')\,\mathrm{d}z')$ can be presented as a sum of rapidly varying and constant parts $c(z) =$
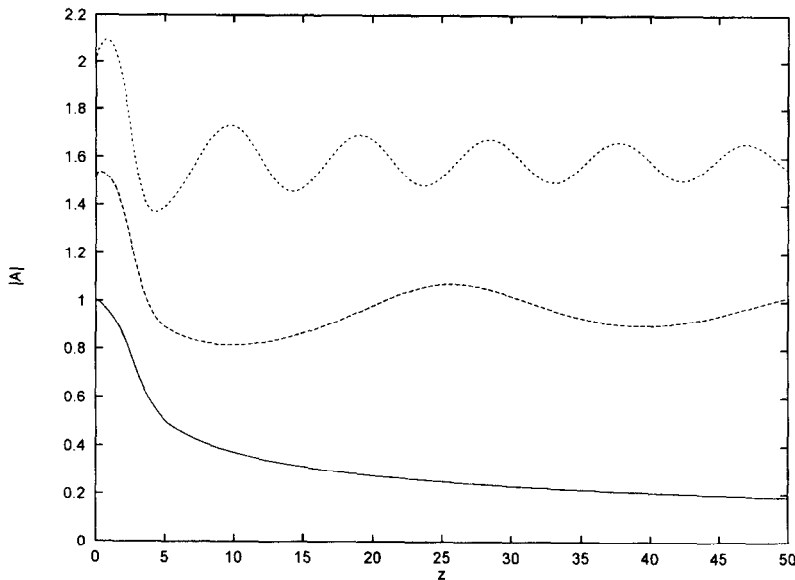

Fig. 10. Nonlinear effects. Pulse amplitude envelope (at maxima) evolution for different initial amplitudes. The Gaussian initial pulse in the form $A(0,t) = B \exp(-t^2)$ is considered. $B = 1$ (solid line); 1.52 (middle curve); 2 (upper curve) and $\langle d \rangle = 0.05$.

$\langle c(z) \rangle + \tilde{c}(z)$, where $\langle \tilde{c}(z) \rangle = 0$ and $\langle c(z) \rangle = [1 - \exp(-2\gamma z_a)]/(2\gamma z_a)$. Here, we use the notation $\langle f \rangle = (1/z_a)\int_0^{z_a} f(z)\,\mathrm{d}z$. We also write $d(z)$ in the similar form $d(z) = \langle d(z) \rangle + \tilde{d}(z)$, where $\langle \tilde{d}(z) \rangle = 0$ and $\langle d \rangle = [d_- z_c + d_+(z_a - z_c)]/z_a$ is a small perturbation due to the average residual dispersion ($\langle d \rangle \approx Z_{\mathrm{dis}}/Z_{\mathrm{DR}} \ll 1$).

Eq. (4) can be derived from the Lagrangian variational principle for the action functional

$$S = \int L \, \mathrm{d}t \, \mathrm{d}z$$

$$= \int \mathrm{d}t \, \mathrm{d}z \left[\frac{i}{2}(Q Q_z^* - Q^* Q_z) + \frac{Z_{\mathrm{NL}}}{2Z_{\mathrm{dis}}} d(z)|Q_t|^2 \right.$$

$$\left. - \frac{c(z)}{2}|Q|^4 \right], \tag{6}$$

which involves the Lagrangian function L. Any solution of Eq. (5) is an extremum of the action S. Therefore, to obtain an approximate model describing the pulse evolution in Eq. (5), one can specify some expected general features of the solution in the trial function, and then obtain a reduced variational problem after the integration on t [20,26,27]. The accuracy of this method depends on how successful the choice of the trial function is, and must be verified by direct numerical integration.

Because the nonlinearity and the residual dispersion act as small perturbations of the linear dynamics, we assume that the pulse dynamics will be close to the structure given by Eq. (3). Therefore, to describe both the rapid pulse-width oscillations and the slow dynamics, which are due to the nonlinearity and the residual dispersion, we chose a trial function in the following form:

$$Q(z,t) = a(z)f[t/b(z)]\exp[i\lambda(z) + i\mu(z)t^2]. \tag{7}$$

After inserting this trial function into Eq. (6), we obtain the reduced variational problem with the action functional

$$\langle S \rangle = \int \langle L \rangle \, \mathrm{d}z, \tag{8}$$

where

$$\langle L \rangle = a^2 b \int |f(s)|^2 \, \mathrm{d}s \, \lambda_z + a^2 b^3 \int s^2 |f(s)|^2 \, \mathrm{d}s \, \mu_z$$

$$+ \frac{Z_{\mathrm{NL}}}{2Z_{\mathrm{dis}}} d(z) \left(a^2 b^{-1} \int |f_s|^2 \, \mathrm{d}s \right.$$

$$\left. + 4\mu^2 a^2 b^3 \int s^2 |f(s)|^2 \, \mathrm{d}s \right)$$

$$- \frac{c(z)}{2} a^4 b \int |f(s)|^4 \, \mathrm{d}s. \tag{9}$$

After a simple calculation, one derives the equations describing the evolution of the parameters $a(z)$, $b(z)$ and $\mu(z)$ (see e.g. Refs. [26,27]).

$$a^2 b = \mathrm{const} = N^2, \tag{10}$$

$$b_z = \frac{2Z_{\mathrm{NL}} d(z)}{Z_{\mathrm{dis}}} b \mu, \tag{11}$$

$$\mu_z + \frac{2Z_{\mathrm{NL}} d(z)}{Z_{\mathrm{dis}}} \mu^2 = \frac{Z_{\mathrm{NL}} d(z) C_1}{2Z_{\mathrm{dis}} b^4} - \frac{c(z) N^2 C_2}{b^3}. \tag{12}$$

Here $C_1 = \int_{-\infty}^{+\infty}|f_x|^2 \, \mathrm{d}x / (\int_{-\infty}^{+\infty} x^2|f|^2 \, \mathrm{d}x)$, $C_2 = \int_{-\infty}^{+\infty}|f|^4 \, \mathrm{d}x / (4\int_{-\infty}^{+\infty} x^2|f|^2 \, \mathrm{d}x)$. For instance, for the soliton shape $f(x) = \mathrm{sech}(x)$, $C_1 = 2C_2 = 4/\pi^2$ and for the Gaussian pulse $f(x) = \exp(-x^2)$, $C_1 = 4$, $C_2 = 1/\sqrt{2}$.

These equations are not yet averaged, so they still include both the fast dynamics due to the variation of dispersion, the losses and the amplification, and the slow dynamics due to the nonlinearity and the residual dispersion. Introducing $\nu = \mu b$ we can obtain from Eqs. (11) and (12)

$$\nu_z = \frac{Z_{\mathrm{NL}} d(z) C_1}{2Z_{\mathrm{dis}} b^3} - \frac{c(z) N^2 C_2}{b^2}. \tag{13}$$

To describe the propagation of the initial pulse, for instance, in the form $A(0,t) = N/\cosh(t)$ we fix the following initial conditions of Eqs. (11) and (13): $b|_{z=0} = 1$ and $\nu|_{z=0} = 0$ (and corresponding C_1 and C_2). The solution of these equations in the linear case (without last term in Eq. (13)) has the form $b_l^2 = 1 + 16R(z)^2/\pi^2$, where $\mathrm{d}R(z)/\mathrm{d}z = d(z)Z_{\mathrm{NL}}/(2Z_{\mathrm{dis}})$. This solution describes the rapid
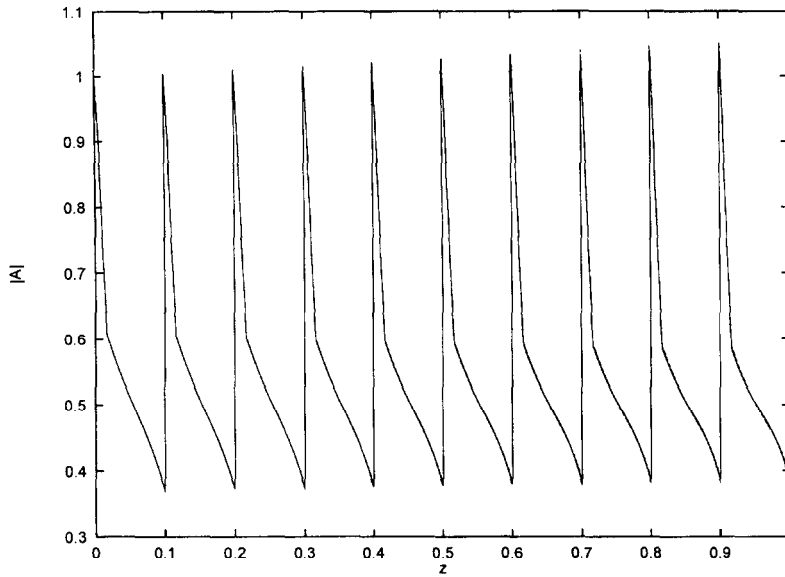
Fig. 11. Comparison of the approximate model and results of direct numerical simulations. Dashed line – oscillations of $|A|$ obtained by variational approach, solid line – direct simulations of Eq. (1). $A(0,t) = \exp(-t^2)$, $\langle d \rangle = 0$.

oscillations due to the variation of the dispersion and the slow broadening due to the residual dispersion. Nonlinear effects and residual dispersion can be considered as perturbations to this solution [20]. To obtain the equation governing small changes of $b(z)$ due to nonlinearity, we linearize Eqs. (11) and (13)
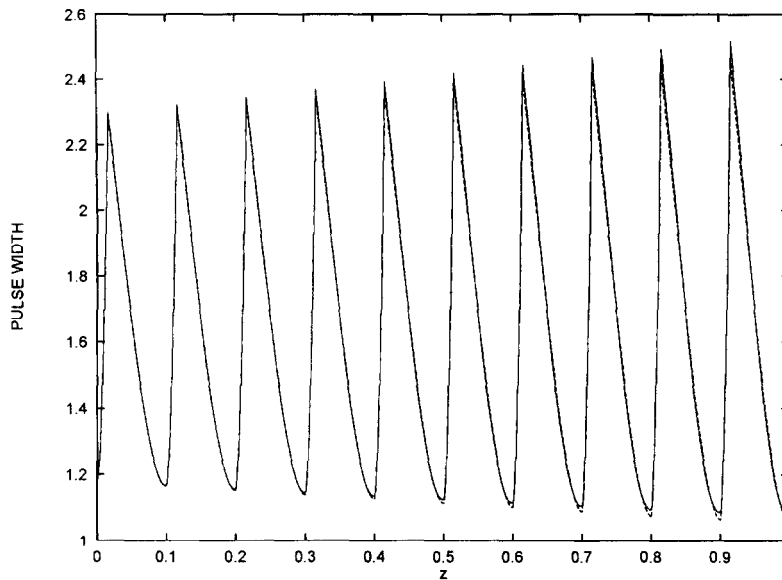

Fig. 12. The same parameters as in Fig. 11 but for the pulse width (FWHM) $T(z)$. Dashed line – oscillations of the $T(z)$ obtained by variational approach, solid line – direct simulations of Eq. (1).

about the linear solution b_l assuming $b = b_l + \tilde{b}_\pm$ and $\tilde{b}_\pm \ll b_l$. Here $\pm$ is for a DCF and SMF respectively.

$$\tilde{b}_z = \frac{2Z_{NL}}{Z_{dis}} d(z) \tilde{\nu},$$

$$\tilde{\nu}_z = -\frac{6Z_{NL} d(z)}{\pi^2 Z_{dis} b_l^4} \tilde{b} - \frac{2c(z)N^2}{\pi^2 b_l^2}. \tag{14}$$

Here and in what follows we drop $\pm$ to avoid complex notation. Initial conditions to Eq. (14) at $z = 0$ are: $\tilde{b} = 0$ and $\tilde{\nu} = 0$. Solution of Eq. (14) with these conditions is found as

$$\tilde{b}_- = -\frac{4Z_{NL} d_- N^2 b_{lz}}{\pi^2 Z_{dis}} \int_0^z \frac{dy}{b_{ly}^2} \int_0^y \frac{c(x)b_{lx}}{b_l^2} \, dx, \tag{15}$$

$$\tilde{b}_+ = r_1 b_{lz} + r_2 b_{lz} \int_{z_c}^z \frac{dy}{b_{ly}^2}$$

$$- \frac{4Z_{NL} d_+ N^2 b_{lz}}{\pi^2 Z_{dis}} \int_{z_c}^z \frac{dy}{b_{ly}^2} \int_{z_c}^y \frac{c(x)b_{lx}}{b_l^2} \, dx. \tag{16}$$

Here b_{lz} denotes time derivative of the linear solution b_l. Coefficients r_1 and r_2 are determined by matching these solutions at $z = z_c$. Resulting change of the pulse width due to nonlinearity over one period in the main order is given by

$$\tilde{b}_+(z_a) = \frac{4N^2 Z_{NL}}{\pi Z_{dis}} \left(d_- \int_0^{z_c} \frac{c(z)z}{b_l^3} \, dz \right.$$

$$\left. - d_+ \int_{z_c}^{z_a} \frac{c(z)(z_a - z)}{b_l^3} \, dz \right). \tag{17}$$

In the case we consider here $d_- < 0$, $d_+ > 0$ and respectively $b_+(z_a) < 0$. One can see that under the above conditions the compression of a pulse ($b_+(z_a) < 0$) due to nonlinear effects can balance dispersive broadening of a pulse due to residual dispersion ($b_{res} > 0$) even on one period. We note, however, that this result was obtained under concrete assumptions concerning the structure of the solution (7).

In Figs. 11, 12 we demonstrate that the variational approach gives a reasonably good approximation of the averaged pulse dynamics for short propagation

distances. The dashed line represents the solution of Eq. (1), and the solid line represents the solution of the variational equations (11) and (12). In Fig. 11 is shown the pulse amplitude evolution and in Fig. 12 the dynamics of the pulse width both computed numerically and calculated from the above variational approach. Difference practically cannot be seen on these scales. This means that a set of ordinary differential equations (11) and (13) gives a rather good approximate description of the breathing dynamics of an optical pulse in links with dispersion compensation on the first stage (short propagation distances). For instance, ten amplifications shown in Figs. 11, 12 correspond to the total propagation distance of 360 km. This means that the variational approach can be used for description of soliton transmission in links of European scales.

3. Conclusion

In conclusion, we have examined numerically and by a variational approach the average optical pulse propagation in cascaded transmission systems with periodic amplification and dispersion compensation. In the span between two amplifiers, a pulse experiences strong attenuation and large width oscillations. We have derived approximate equations describing the pulse-amplitude and width oscillations, and found that the results obtained by this approach for short propagation distances are in good agreement with the results of direct numerical computations. We have demonstrated numerically that a bright soliton can propagate in a fiber system that includes segments with high normal dispersion.

It should be pointed out that stable propagation of "bright" pulses is possible only if the residual dispersion coefficient D_{res} is positive (anomalous dispersion region). The results of our numerical simulations confirm the possibility of "breathing" pulse transmission.

References

[1] L.F. Mollenauer, S.G. Evangelides, Jr. and H.A. Haus, IEEE J. Lightwave Tech. 9 (1994) 194.

[2] M. Nakazawa and H. Kubota, Electron. Lett. 31 (1995) 216.

[3] L.F. Mollenauer, P.V. Mamyushev and M.J. Neubelt, Optics Lett. 19 (1995) 704.

[4] L.F. Mollenauer, P.V. Mamyshev and M.J. Neubert, Demonstration of soliton WDM transmission at up to 8X10Gbit/s, error-free over transoceanic distances, Post Deadline presentation, PD22-1, OFC'96, San Jose.

[5] A. Hasegawa and Y. Kodama, Optics Lett. 15 (1990) 1444; Phys. Rev. Lett. 66 (1991) 161.

[6] K.J. Blow and N.J. Doran, IEEE Photon. Technol. Lett. 3 (1991) 369.

[7] C. Lin, H. Kogelnik and L.G. Cohen, Optics Lett. 5 (1980) 476.

[8] R. Kashyap, Optical Fiber Technology 1 (1994) 17.

[9] U. Peschel, T. Peschel and F. Lederer, Appl. Phys. Lett. 67 (1995) 2111.

[10] H. Onaka, H. Miyta, K. Otsuka and T. Chikama, Proc. ECOC, Vol. 4 (1994) p.49.

[11] C.D. Chen, J-M.P. Delavaux, B.W. Hakki, O. Mizuhara, T.V. Nguyen, R.J. Nuyts, K. Ogawa, Y.K. Park, R.E. Tench, L.D. Tzeng and P.D. Yeates, Electron. Lett. 30 (1994) 1159.

[12] A.D. Ellis and D.M. Spirit, Electron. Lett. 30 (1994) 72.

[13] C. Das, U. Gaubatz, E. Gottwald, K. Kotten, F. Küppers, A. Mattheus and C.J. Weiske, Electron. Lett. 31 (1995) 305.

[14] C. Das, B. Hein, U. Gaubatz, E. Gottwald, K. Kotten, F. Küppers, A. Mattheus, L. Rapp and C.J. Weiske, Proc. OFC (1995) San Diego.

[15] F. Nidemaier, A. Mattheus and R. Ries, Proc. COST Workshop, Nizza, 1994, p. 45.

[16] I. Gabitov and S.K. Turitsyn, Optics Lett. 21 (1995) 327; Averaged pulse dynamics in the cascaded transmission systems with a passive dispersion compensation, Preprint Los Alamos, LAUR-95-3633, 1995.

[17] I. Gabitov, F. Küppers, A. Mattheus and S. Turitsyn, Averaged pulse dynamics in cascaded passive fiber compensated transmission system, Preprint Los Alamos, LAUR-95-2230, 1995.

[18] F.M. Knox, W. Forysiak and N.J. Doran, IEEE J. Lightwave Technology 13 (1995) 1955.

[19] N. Smith, F.M. Knox, N.J. Doran, K.J. Blow and Bennion, Electron. Lett. 32 (1995) 55.

[20] I. Gabitov and S.K. Turitsyn, Pisma JETP 63 (1996) 814.

[21] B. Malomed, D. Parker and N. Smyth, Phys. Rev. E 48 (1993) 1418.

[22] R. Grimshaw, J. He and B. Malomed, Physica Scripta 53 (1996) 385.

[23] M. Nakazawa and H. Kubota, Japan J. Appl. Phys. 34 (1995) L681.

[24] A. Mattheus and S.K. Turitsyn, Pulse interaction in nonlinear communication systems based on standard monomode fibres, Proc. ECOC, Vol. 2 (1994) p. 37.

[25] G.P. Agrawal, Nonlinear Fiber Optics (Academic, San Diego, 1989).

[26] D. Anderson, Phys. Rev. A 27 (1983) 3135; D. Anderson and M. Lisak, Optics Lett. 10 (1985) 390.

[27] D. Anderson and M. Lisak, Optics Lett. 10 (1985) 134; D. Anderson, M. Lisak, B. Malomed and M. Quiroga-Teixeiro, J. Opt. Soc. Am. B 11 (1994) 2380; B. Malomed, Optics Lett. 19 (1994) 341; D. Anderson, M. Lisak and T. Reichel, J. Opt. Soc. Am. B 5 (1988) 207.